Original Article
High-risk HPV E6/E7 mRNA in situ hybridization in endocervical glandular neoplasia: performance compared with p16^{INK4a} and Ki67 immunochemistry

Tingting Chen[*], Jing Li[*], Shunni Wang, Yan Ning, Xianrong Zhou, Yiqin Wang

Department of Pathology, Obstetrics and Gynecology Hospital of Fudan University, No. 128, Shenyang Road, Shanghai 200082, China. [*]Equal contributors.

Abstract: Objective: HR-HPV E6/E7 mRNA in situ hybridization (HR-HPV RISH) can detect HPV-driven endocervical glandular neoplasia. Our aim was to compare its diagnostic performance with the conventional p16^{INK4a} and Ki67 immunochemistry (IHC). Methods: HR-HPV RISH and IHC were performed in normal cervix (n = 70), reactive cervix (n = 60), adenocarcinoma in situ (AIS) (n = 92), endocervical adenocarcinoma (ECA) and adenosquamous carcinoma (n = 21) samples (n = 163). The sensitivities and specificities of the three markers were compared in the benign, AIS, HPV-associated adenocarcinoma (HPVA) and non HPV-associated adenocarcinoma (NHPVA) samples, and in 39 endocervical curettage specimens containing endometrial and HPV-associated neoplastic glands. Finally, the inter-observer agreement rate for the three markers were calculated. Results: The sensitivities of HR-HPV RISH, P16^{INK4a} and Ki67 were 100% for the HPV-related glandular neoplasia and HPVAs in ECAs, while the specificity of HR-HPV RISH (100%) were higher than the other two (88.89% and 17.77% for P16^{INK4a} and Ki67 respectively) in the HPVAs. Furthermore, HR-HPV RISH was more specific than either p16^{INK4a} block+ or Ki67 in the endocervical curettage specimens and in HPVAs with poor differentiation. Finally, the inter-observer agreement for HR-HPV RISH was higher than that for the morphological, p16^{INK4a} block+ and Ki67 markers (99.67% vs. 95.10%, 99.35% and 90.85% respectively). Conclusions: HR-HPV RISH is highly sensitive and specific for HPV-driven endocervical glandular neoplasia compared to p16^{INK4a} and Ki67, and should be incorporated for ECA diagnosis.

Keywords: Cervical glandular neoplasia, HR-HPV, mRNA RISH, P16^{INK4a}, Ki67

Introduction

High-risk human papillomaviruses (HR-HPVs) are the cause of nearly all cervical squamous cell carcinomas and more than 75% of the endocervical adenocarcinomas (ECAs) [1, 2]. Despite the ambiguous correlation between HR-HPV infection and the carcinogenic mechanisms of ECAs, the International Endocervical Adenocarcinoma Criteria and Classification (IECC) recommends evaluating the HPV status prior to the conventional morphological classification, since the HPV-associated adenocarcinomas (HPVAs) show better prognosis than the non-HPV adenocarcinomas (NHPVAs) [3]. Therefore, accurate detection of HR-HPVs in the cervical glandular malignancies is crucial for predicting the prognosis of ECAs.

Presence of p16^{INK4a}/Ki67 is a surrogate marker of HR-HPV infection in the HPV-associated endocervical neoplasias [4, 5]. However, the scoring system of p16^{INK4a} is at present controversial, and often leads to misinterpretation of the staining results [6, 7], while the diagnostic value of Ki67 in ECAs is still ambiguous. Based on the tumorigenic significance of the highly type-specific E6 and E7 genes of HR-HPVs in cervical squamous cell carcinomas [8, 9], E6/E7 mRNA *in situ* hybridization (HR-HPV RISH) has been developed to detect type-specific HR-HPVs [10-12]. A recent study also showed that HR-HPV RISH effectively diagnosed HPVAs [13]. The aim of our study was to compare the diagnostic efficiencies of RISH and p16^{INK4a}/Ki67 immunohistochemistry (IHC) by testing their performance in normal and reactive cervi-

cal tissues, as well as in adenocarcinoma in situ (AIS), ECA subtypes and adenosquamous carcinomas.

Material and methods

Case selection

A total of 406 formalin-fixed paraffin-embedded (FFPE) cervical tissue blocks were collected from August 1st 2017 to March 31st 2019 at the Obstetrics and Gynecology Hospital of Fudan University, which included samples of normal cervix (n = 70), reactive cervix (n = 60), AIS (n = 92), ECA (n = 163) and adenosquamous carcinomas (n = 21). Samples from patients who had received preoperative neoadjuvant chemotherapy and/or radiotherapy were excluded. Depending on the procedure, samples included 117 from endocervical curettage and cervical biopsies, 80 from loop electrosurgical excision procedure (LEEPs), and 201 from hysterectomies or radical hysterectomies. All patients signed the written informed consent, and the study was approved by the ethics committee of Obstetrics and Gynecology Hospital of Fudan University. The tissue blocks were cut into sections for the following assays: (1) H&E staining for morphological identification, (2) p16^{INK4a} IHC, (3) Ki67 IHC, (4) HR-HPV RISH, (5) DapB RISH (negative control), (6) Hs-PPIB RISH (housekeeping/positive control), and (7) IHC for p53, Napsin-A and HNF-1β for subtype identification.

Morphological evaluation

Two senior pathologists reviewed the H&E stained slides independently, and any ambiguity was resolved by co-examination using a multi-head microscope. Based on the IECC and WHO 2014 criteria, the usual (n = 109), mucinous-not otherwise specified (NOS) (n = 6) and mucinous-intestinal (n = 3) types were classified as HPVAs, while the endometrioid (n = 2), mucinous gastric (n = 36), serous (n = 2) and clear cell (CCC, n = 3) types as NHPVAs. The morphological criteria for the gastric type were based on the existing as well as revised recommendations [14], which also include the minimal deviation adenocarcinoma. All patients diagnosed with the endometrioid, gastric, serous and CCC subtypes underwent radical hysterectomy along with salpingo-oophorectomy. The diagnoses of these subtypes were deter-

mined after excluding the possibility of other original sites by the sufficient sampling of endometrium, fallopian tubes and ovaries.

Immunochemistry (IHC)

IHC was performed as per standard protocols, and the antibodies used to target p16^{INK4a}, Ki67, p53, Napsin-A and HNF-1β are listed in Table S1. PBS buffer was used in lieu of the primary antibody as a negative control. The IHC results were analyzed independently by two pathologists blinded to the samples. The p16^{INK4a} staining pattern was classified as negative (no staining), patchy (patchy+, focal and uneven staining in the nuclei and cytoplasm) and block-like (block+, diffuse and even staining in the nuclei and cytoplasm in 100% of the tumor cells). For Ki67, the cells with nuclear staining were counted in at least 10 fields per slide and the average was calculated.

Human papillomavirus E6/E7 RNA in situ hybridization (HR-HPV RISH)

HR-HPV RISH was performed using the RNA scope 2.5 HD Detection Reagent-BROWN (#322310, Advanced Cell Diagnostics, USA) and Multiplex Fluorescent (#323100) according to the manufacturer's instructions. The DapB probe (#310043) was used as the negative control and Hs-PPIB (#313901) as the positive control. Probe-HPV-HR18 (16, 18, 26, 31, 33, 35, 39, 45, 51, 52, 53, 56, 58, 59, 66, 68, 73, and 82) (#312591) was used for the test samples. Images were taken at 40× magnification using the BX45 (Olympus, Japan) light microscope, Leica inverted fluorescence microscope with ProgRes Image Capture Software (JENOPTIK Optical System, Jena, German) & Leica Confocal LAS-AF SP5 System. Dark-brown, punctuate dots in the nucleus and/or cytoplasm under the light microscope, and green (Fluor 488) signals under the fluorescence systems were considered positive. The HR-HPV RISH slides were evaluated by two pathologists blinded to the morphological diagnoses in order to exclude any possible influences of the morphology.

Statistical analysis

All statistical analyses were performed using SPSS 20.0 (SPSS, IBM). The Student t-test and one-way ANOVA were used to compare Ki67

Table 1. Expressions of RISH, P16^{INK4a} and Ki67 performances in benign and neoplastic cervical glands

Lesion	N^a (385)	RISH+	p16			Ki67	Ki67 ≥ 10%+	RISH+/P16 (block+)	RISH+/Ki67 ≥ 10%+
			0	Patchy+	Block+				
Normal	70	0	69	1	0	1.57 ± 2.07 (0.00-5.00)	0	0/0	0/0
Reactive	60	0	34	26	0	7.40 ± 6.20 (0.00-30.00)	17	0/0	0/17
AIS	92	92	0	0	92	34.53 ± 14.78 (15.00-80.00)*	92	92/92	92/92
ECA total	163	118	30	10	123	39.56 ± 21.15 (5.00-90.00)*	155	118/123	89/155
HPVAs									
Usual type	109	109	0	0	109	47.55 ± 18.10 (20.00-90.00)	109	109/109	109/109
Mucinous, NOS	6	6	0	0	6	45.00 ± 22.80 (15.00-70.00)	6	6/6	6/6
Mucinous, Intestinal^b	3	3	0	0	3	36.67 ± 5.77 (30.00-40.00)	3	3/3	3/3
NHPVAs									
Endometrioid	2	0	0	2	0	27.50 ± 17.68 (15.00-40.00)	2	0/0	2/2
Mucinous, Gastric	36	0	30	6	0	16.38 ± 10.80 (5.00-50.00)	28	0/0	0/28
Serous	2	0	0	0	2	65.00 ± 7.07 (60.00-70.00)	2	0/2	0/2
CCC	3	0	0	2	1	25.00 ± 8.66 (15.00-30.00)	3	0/1	0/3
Adenocarcinoma, NOS	2	0	0	0	2	15.00 ± 7.07 (10.00-20.00)	2	0/2	0/2

^{a}The cases of adenosquamous carcinoma (n = 21) were not included. ^{b}The mucinous-intestinal subtype was confirmed by excluding the diagnosis of usual and the mucinous-NOS subtypes. *One-way ANOVA, $P < 0.01$.
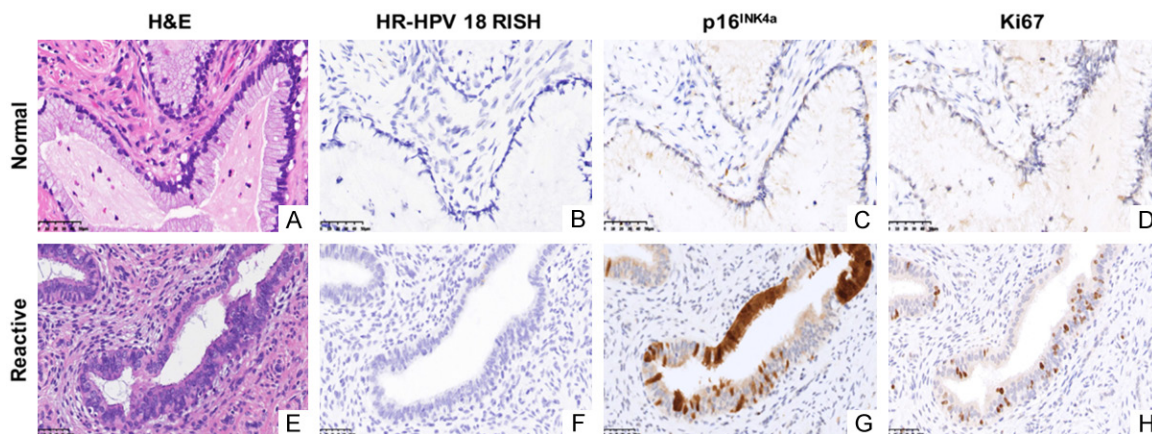

Figure 1. HR-HPV RISH, p16^{INK4a} and Ki67 expressions in the normal and reactive cervical glands. The representative images of H&E, HR-HPV RISH, p16^{INK4a} and Ki67 expressions in the normal (A-D) and reactive (E-H) cervical glands. Scale bars = 50 μm.

between two or multiple groups. The *Kappa* coefficient test was used to analyze the interobserver agreement. $P < 0.05$ was considered statistically significant.

Results

None of the normal and reactive cervix samples were positive for HR-HPV RISH+ or p16^{INK4a} block+ (**Table 1**; **Figure 1**), while 1/70 (1.43%) of the normal cervix and 26/60 (43.33%) of the reactive cervix samples showed p16^{INK4a} patchy+ staining (**Table 1**; **Figure 1**). The average Ki67 positive rates in the normal and reactive samples were 1.57% ± 2.07% and 7.40% ± 6.2% respectively, which were significantly lower than that in the AIS (34.53% ± 14.78%) and

invasive adenocarcinoma (39.56% ± 21.15%) samples ($P < 0.01$, **Table 1**). Within the ECAs, the average Ki67 positive rates of the adenocarcinoma-NOS (15% ± 7.07%) and gastric (16.38% ± 10.8%) types were significantly lower compared to the other types, but higher than that of the normal/reactive samples ($P < 0.01$, **Table 1**). Therefore, we chose Ki67 ≥ 10% as the cutoff value for demarcating samples into Ki67+ or Ki67- (**Table 1**); based on this criteria, all normal cervix samples were negative and only 17/60 of the reactive samples (28.33%) were positive (**Table 1**).

All AIS samples were HR-HPV RISH+/p16^{INK4a} block+/Ki67+ (**Figures 2** and <u>S1</u>), as were the usual, mucinous-NOS and mucinous-intestinal
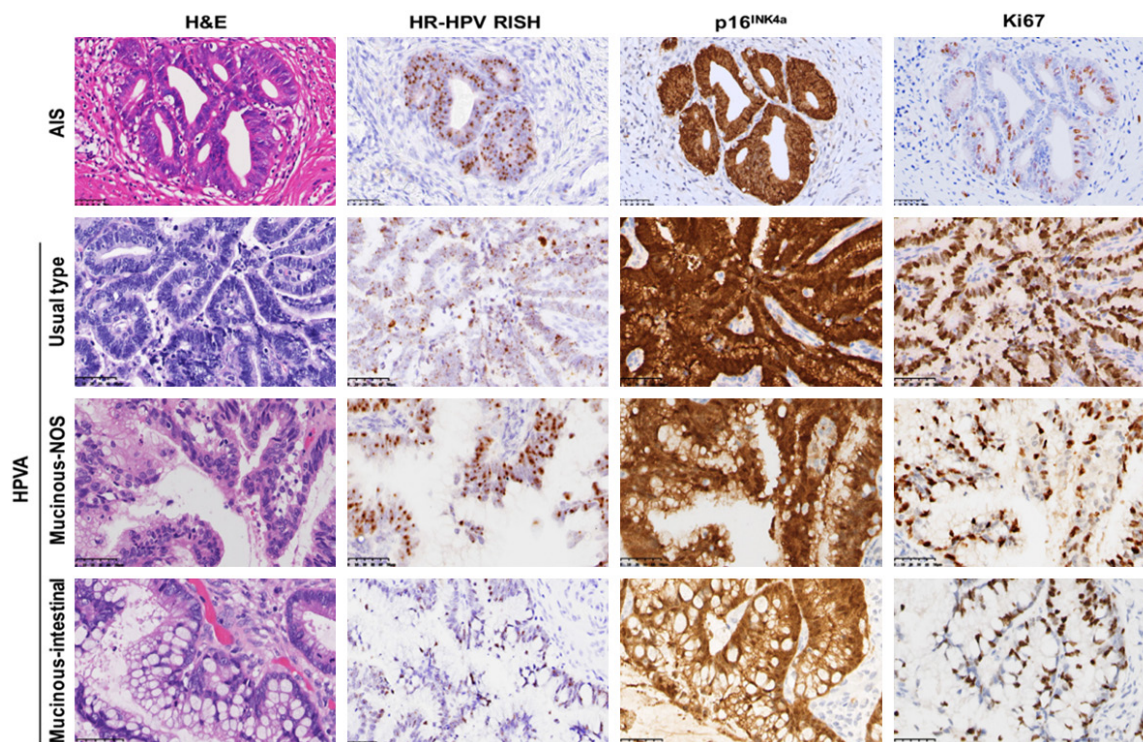
Figure 2. HR-HPV RISH, p16^{INK4a} and Ki67 performances in the endocervical HPV-associated adenocarcinomas (HP-VAs). The representative images of H&E, HR-HPV RISH, p16^{INK4a} and Ki67 expressions in the AIS and HPVAs: usual type, mucinous-NOS type and mucinous-intestinal type. Scale bars = 50 μm. AIS: adenocarcinoma in situ; NOS: not otherwise specified; ECA: endocervical adenocarcinoma; HPVA: HPV-associated adenocarcinoma.

HPVAs (**Table 1** and **Figures 2** and S1), and the adenosquamous carcinoma samples (Figure S2).

Not surprisingly, all the NHPVAs were HR-HPV RISH- (**Figure 3**).

In addition, 100% of the mucinous-gastric type and endometrioid types were p16^{INK4a}-, although 100% of the endometrioid and 16.67% of the mucinous-gastric type ECAs still presented some patchy p16^{INK4a} staining, while 100% of the serous and 33.33% of the CCC types were p16^{INK4a} block+ (**Table 1**; **Figure 3**). All endometrioid, serous and CCC adenocarcinomas were Ki67+, while 22.22% of the mucinous-gastric ECAs were Ki67- (**Table 1**; **Figure 3**). Furthermore, 100% of the serous adenocarcinoma were p53+ (**Figure 3**), and all the CCC types were HNF-1β+ and Napsin-A+ (Figure S3). Two cases classified as adenocarcinoma NOS were HR-HPV RISH-/p16^{INK4a}-/Ki67+. Interestingly, the histological diagnosis of 2 cases was contradicted by the molecular features: a sample diagnosed as the serous type on account of severe nuclear atypea and papillary-like growth pattern (**Figure 4A**) was identified as HR-HPV RISH+/p16^{INK4a} block+/p53 wild-type/Ki67+ (**Figure 4B-E**), and another diagnosed as the CCC type for its tubule-cystic growth pattern and clear cell-like changes (**Figure 4F**) exhibited HR-HPV RISH+/p16^{INK4a} block+/Napsin-A-/HNF-1β- (**Figures 4G-J**, S3). Therefore, both cases were re-classified as HPVAs of usual type with poor differentiation.

The overall sensitivity of HR-HPV RISH in cervical glandular neoplasia was 82.35%, which was lower than that of either p16^{INK4a} (block+: 84.31%; patchy+/block+: 88.24%) or Ki67+ (96.86%) (**Table 2**), while the specificities of all markers were similar (HR-HPV RISH: 100%; p16^{INK4a} block+: 100%; Ki67+: 86.92%, p16^{INK4a} patchy+/block+: 80%; **Table 2**). The sensitivities of all three markers for HPV-related neoplasia and HPVAs were 100% (**Table 2**), but the specificity of HR-HPV RISH (100%) was superior to that of p16^{INK4a} (block+: 88.89%; patchy+/block+: 66.67%, **Table 2**) as well as Ki67+ (17.77%, **Table 2**).
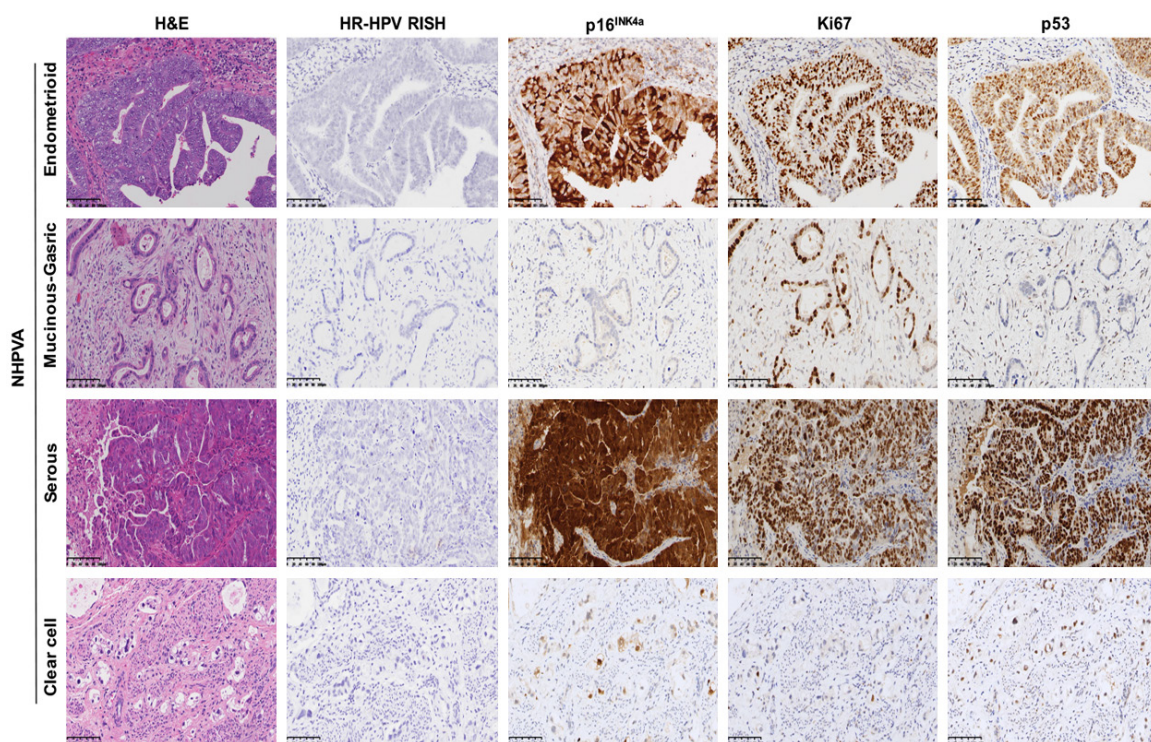
Figure 3. HR-HPV RISH, p16^{INK4a} and Ki67 performances in the endocervical non HPV-associated adenocarcinomas (NHPVAs). The representative images of H&E, HR-HPV RISH, p16^{INK4a}, Ki67 and p53 expressions in the adenocarcinoma of endometrioid type, mucinous-gastric type, serous type and clear cell type. Scale bars = 100 μm.
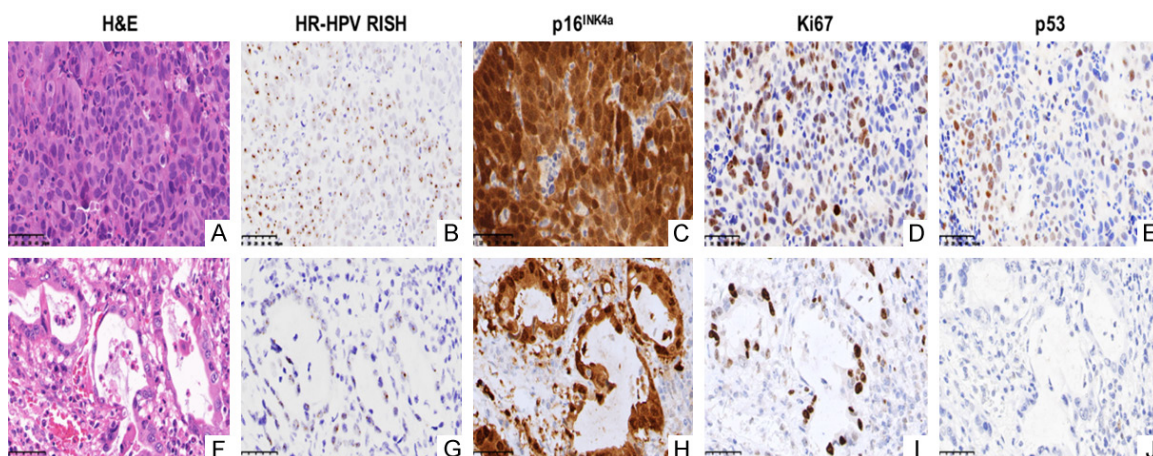

Figure 4. HR-HPV RISH, p16^{INK4a} and Ki67 performances in the poor-differentiated HPVAs. The representative images of H&E, HR-HPV RISH, p16^{INK4a}, Ki67 and p53 expressions in the HPVAs with poor differentiation. Scale bars = 50 μm. HPVA: HPV associated adenocarcinoma.

We also assessed the performance of HR-HPV RISH, p16^{INK4a} and Ki67 in the endocervical curettage specimens containing the HPV-related neoplastic glands and proliferative endometrium. In 39 endocervical curettage specimens (31 AIS and 8 HPVAs), the morpho-logical features of the neoplastic cervical glands mimicked the proliferative endometrial glands (**Figure 5A-C**). While 100% of the endometrioid glands were p16^{INK4a} patchy+, 100% of the HPV-related neoplastic endocervical glands were p16^{INK4a} block+ (**Table 3**; **Figure**

Table 2. The comparison of sensitivities and specificities of the detected markers

| Marker	Sensitivity (%) Overall neoplasia	Specificity (%) Overall neoplasia	Sensitivity (%) HPV-related neoplasia	Sensitivity (%) HPVA in ECAs	Specificity (%) HPVA in ECAs
HR-HPV RISH	82.35% (210/255)	100% (130/130)	100% (210/210)	100% (118/118)	100% (45/45)
IHC of p16^{INK4a} (patchy+/block+)	88.24% (225/255)	80.00% (104/130)	100% (210/210)	100% (118/118)	66.67% (30/45)
IHC of p16^{INK4a} (block+ only)	84.31% (215/255)	100% (130/130)	100% (210/210)	100% (118/118)	88.89% (40/45)
IHC of Ki67 ≥ 10%+	96.86% (247/255)	86.92% (113/130)	100% (210/210)	100% (118/118)	17.77% (8/45)
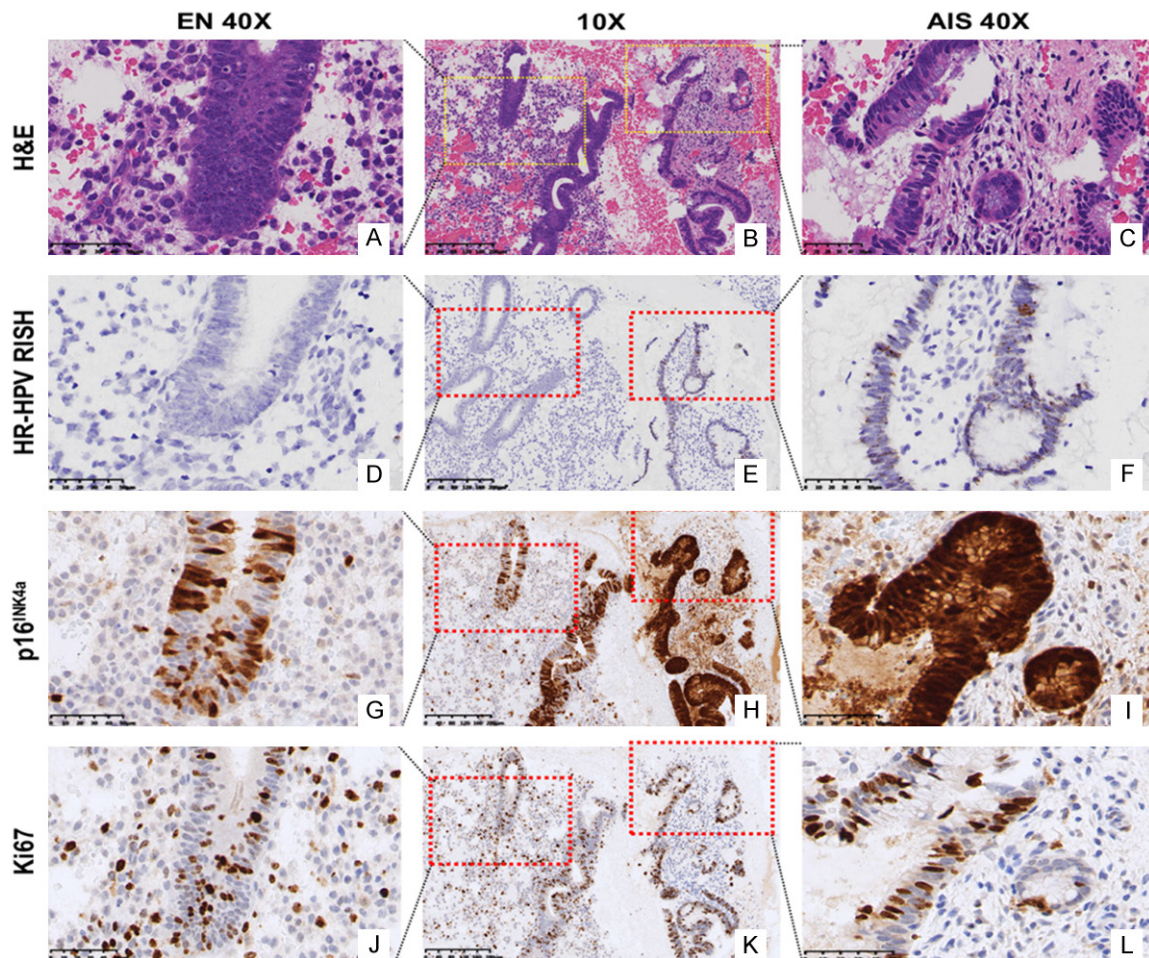
Figure 5. HR-HPV RISH, p16^{INK4a} and Ki67 performances in the endocervical curettage specimens. The representative images of endometrial glands and HPV-related neoplastic cervical glands in the curettage specimens. Each parts were also shown under high magnification separately. (B, E, H and K): Scale bars = 200 μm. (A, C, D, F, G, I, J and L): Scale bars = 50 μm.

5G-I). In addition, 100% of the neoplastic cervical glands and 87.18% of the proliferative endometrium were Ki67+ (**Table 3**), and the average Ki67 positive rates were similar in the proliferative endometrial glands and neoplastic glands (21.43% ± 7.57% vs. 34.89% ± 15.15%) (**Figure 5J-L**). However, all endometrial glands were negative for HR-HPV RISH, while all the HPV-related neoplastic endocervical glands were HR-HPV RISH+ (**Table 3**; **Figure 5D-F**).

There was 95.1% inter-observer agreement between the two pathologists regarding the presence of glandular neoplasia (K = 0.934; 95% CI: 0.900-0.967), and that for HR-HPV RISH was near perfect at 99.67% (K = 0.993; 95% confidence interval, 0.979-1.006). The inter-observer agreement for Ki67+, p16^{INK4a} (patchy+/block+) and p16^{INK4a} block+ only were respectively 90.85% (K = 0.810; 95% CI: 0.743-0.877), 91.5% (K = 0.852, 95% CI: 0.799-

Table 3. Comparison of HR-HPV RISH, p16^{INK4a} and Ki67 IHC in 39 endocervical curettage specimens

| Histology | N | RISH+ | p16+ score | | | Ki67 | Ki67 ≥ 10%+ | RISH+/P16 (Patchy+/ Block+) | RISH+/ Ki67 ≥ 10%+ |
			0	Patchy+	Block+				
Proliferative Endometrial	39	0	0	39	0	21.43% ± 7.57% (10.00-35.00)	34	0/39	0/39
AIS/HPVA	39	39	0	0	39	34.89% ± 15.15% (15.00-60.00)*	39	39/39	39/39

*Paired student's t-test, $P < 0.01$.

0.901) and 99.35% (K = 0.987, 95% *CI*: 0.969-1.005).

Discussion

Compared to p16^{INK4a} and Ki67 IHC, HR-HPV RISH showed a similar sensitivity of 100% but higher specificity for the HPV-related cervical neoplasia. In addition, HR-HPV RISH showed superior ability to discriminate between curettage specimens and HPVAs with poor differentiation. Therefore, HR-HPV RISH has a distinct diagnostic advantage for ECAs.

The 2014 version of the WHO classification system for ECAs is based on histological features and IHC, which identifies several subtypes including usual, mucinous, endometrioid, serous, CCC etc. Recent evidence also points to an HPV-driven influence on the clinical outcomes of these subtypes. IECC recently reclassified ECAs into HPVAs and NHPVAs on the basis of both morphology (compatible with the 2014 WHO classification) and etiology [13]. Stolnicu et al. found that HPVAs showed superior overall survival, disease-free survival and progression-free survival compared to the NHPVAs, indicating that detection of HR-HPVs can significantly affect the clinical outcomes of ECAs [3].

The conventional p16^{INK4a} and Ki67 panel is highly sensitive and relatively specific to endocervical neoplasia [5, 15], and can partly predict HPV association. However, Ki67 positivity is highly dependent on reactive changes and cell proliferation [16, 17]. In our study, Ki67 showed the highest sensitivity for cervical glandular neoplasia compared to the other two markers. However, since 28.33% of the reactive cervix samples and 87.18% of the proliferative endometrium samples were also positive for Ki67, it reduced the specificity of the ≥ 10% cutoff. Furthermore, the Ki67 status had the lowest inter-observer agreement in our study. Similarly, the inconsistent scoring system of

p16^{INK4a} has also led to misdiagnosis in previous studies [18]. Han *et al.* designed a scoring system from 0 to 12 for p16^{INK4a} in the ECAs [19], while McCluggage set the scores from 0 to 9 [7]. Until recently, IECC recommended that only p16^{INK4a} block+ be considered positive [13]. In our study, the sensitivity and specificity of p16^{INK4a} block+ was 100% for all the HPV-related endocervical glandular neoplasia with a relatively excellent inter-observer agreement. However, its specificity for HPVAs in ECAs was only 88.89%. Furthermore, the combination of Ki67 and p16^{INK4a} failed to distinguish HPVAs with poor differentiation (**Figure 3**). Taken together, p16^{INK4a} block+ is a sensitive marker for cervical glandular neoplasia, but a deficient surrogate for HPVAs.

HR-HPV RISH is a robust technique for HR-HPV diagnosis [12, 13], and detects the full-length or fragments of E6 and E7 transcripts using cascade signal amplification [12, 20]. Studies show that persistent infection with HR-HPVs results in integration of the viral genome fragments into host chromosomes, thus facilitating the transcription of type-specific E6/E7 genes and protein overexpression, which eventually activate the downstream carcinogenetic signaling pathways [21, 22]. Therefore, the high specificity of HR-HPV RISH for HPV-driven cervical neoplasia is expected. In this study, HR-HPV RISH was highly sensitive and specific for cervical glandular neoplasia and HPVAs in ECAs, and unaffected by reactive changes or the NHPVA subtypes. Furthermore, the inter-observer agreement rate for HR-HPV RISH was the highest at 99.67%, making HR-HPV a reliable marker for HPV-driven cervical neoplasia. Considering the significant difference in the survival of HPVA and NHPVA patients [3], the inclusion of HR-HPV RISH could contribute to the multimodal therapy of ECAs.

Based on our results, we strongly recommend HR-HPV RISH to distinguish AIS from reactive cervix, since the latter can mimic AIS with mild

nuclear enlargement, increased nucleus/cyto-plasm ratio and visible mitotic figures. The p16^{INK4a}/Ki67 expression pattern is usually ambiguous in these lesions (**Figure 1**). Secondly, HR-HPV RISH can discriminate AIS from the endometrium in endocervical curettage specimens, while p16^{INK4a} and Ki67 staining in the endometrial epithelium can confound the HPV+ status in neoplastic cervical glands [23] (**Figure 5**). Finally, unlike p16^{INK4a}/Ki67 IHC, HR-HPV RISH can distinguish poorly differentiated HPVAs from HPVAs (**Figure 4**). Further studies have to be conducted on larger cohorts to validate our findings.

Conclusion

HR-HPV RISH is a highly sensitive and specific technique for HPV-associated endocervical glandular neoplasia, and can supplement differential diagnosis of HPVAs currently used in clinical practice.

Acknowledgements

Disclosure of conflict of interest

None.

Address correspondence to: Dr. Yiqin Wang, Department of Pathology, Obstetrics and Gynecology Hospital of Fudan University, No. 419, Fang-Xie Road, Shanghai 200082, China. Tel: +86 021 63455050-8384; E-mail: yiqinwang11@fudan.edu.cn

References

[1] Stolnicu S, Hoang L, Hanko-Bauer O, Barsan I, Terinte C, Pesci A, Aviel-Ronen S, Kiyokawa T, Alvarado-Cabrero I, Oliva E, Park KJ and Soslow RA. Cervical adenosquamous carcinoma: detailed analysis of morphology, immunohistochemical profile, and clinical outcomes in 59 cases. Mod Pathol 2019; 32: 269-279.

[2] Siegel RL, Miller KD and Jemal A. Cancer statistics, 2019. CA Cancer J Clin 2019; 69: 7-34.

[3] Stolnicu S, Hoang L, Chiu D, Hanko-Bauer O, Terinte C, Pesci A, Aviel-Ronen S, Kiyokawa T, Alvarado-Cabrero I, Oliva E, Park KJ, Abu-Rustum NR and Soslow RA. Clinical outcomes of HPV-associated and unassociated endocervical adenocarcinomas categorized by the international endocervical adenocarcinoma criteria and classification (IECC). Am J Surg Pathol 2019; 43: 466-474.

[4] Missaoui N, Hmissa S, Frappart L, Trabelsi A, Ben Abdelkader A, Traore C, Mokni M, Yaacoubi MT and Korbi S. p16INK4A overexpression and HPV infection in uterine cervix adenocarcinoma. Virchows Arch 2006; 448: 597-603.

[5] Muller S, Flores-Staino C, Skyldberg B, Hellstrom AC, Johansson B, Hagmar B, Wallin KL and Andersson S. Expression of p16INK4a and MIB-1 in relation to histopathology and HPV types in cervical adenocarcinoma. Int J Oncol 2008; 32: 333-340.

[6] Ishikawa M, Fujii T, Saito M, Nindl I, Ono A, Kubushiro K, Tsukazaki K, Mukai M and Nozawa S. Overexpression of p16 INK4a as an indicator for human papillomavirus oncogenic activity in cervical squamous neoplasia. Int J Gynecol Cancer 2006; 16: 347-353.

[7] McCluggage WG and Jenkins D. p16 immunoreactivity may assist in the distinction between endometrial and endocervical adenocarcinoma. Int J Gynecol Pathol 2003; 22: 231-235.

[8] Callejas-Valera JL, Iglesias-Bartolome R, Amornphimoltham P, Palacios-Garcia J, Martin D, Califano JA, Molinolo AA and Gutkind JS. mTOR inhibition prevents rapid-onset of carcinogen-induced malignancies in a novel inducible HPV-16 E6/E7 mouse model. Carcinogenesis 2016; 37: 1014-1025.

[9] Fontecha N, Basaras M, Hernaez S, Andia D and Cisterna R. Assessment of human papillomavirus E6/E7 oncogene expression as cervical disease biomarker. BMC Cancer 2016; 16: 852.

[10] Mills AM, Coppock JD, Willis BC and Stoler MH. HPV E6/E7 mRNA in situ hybridization in the diagnosis of cervical low-grade squamous intraepithelial lesions (LSIL). Am J Surg Pathol 2018; 42: 192-200.

[11] Zhan X, Wang S, Wu X, Qiu X, Li F, Zeng Y and Chen Z. The role of HPV E6/E7 mRNA combined with P16/ki67 immunocytochemistry in the diagnosis of atypical squamous cells of undetermined significance (ASCUS). Xi Bao Yu Fen Zi Mian Yi Xue Za Zhi 2018; 34: 937-941.

[12] Mills AM, Dirks DC, Poulter MD, Mills SE and Stoler MH. HR-HPV E6/E7 mRNa in situ hybridization: validation against PCR, DNA in situ hybridization, and p16 immunohistochemistry in 102 samples of cervical, vulvar, anal, and head and neck neoplasia. Am J Surg Pathol 2017; 41: 607-615.

[13] Stolnicu S, Barsan I, Hoang L, Patel P, Terinte C, Pesci A, Aviel-Ronen S, Kiyokawa T, Alvarado-Cabrero I, Pike MC, Oliva E, Park KJ and So-

slow RA. International endocervical adenocarcinoma criteria and classification (IECC): a new pathogenetic classification for invasive adenocarcinomas of the endocervix. Am J Surg Pathol 2018; 42: 214-226.

[14] Talia KL and McCluggage WG. The developing spectrum of gastric-type cervical glandular lesions. Pathology 2018; 50: 122-133.

[15] Oka K, Nakano T and Hoshi T. Analysis of response to radiation therapy of patients with cervical adenocarcinoma compared with squamous cell carcinoma. MIB-1 and PC10 labeling indices. Cancer 1996; 77: 2280-2285.

[16] Goel MM and Mehrotra A. Immunohistochemical expression of MIB-1 and PCNA in precancerous and cancerous lesions of uterine cervix. Indian J Cancer 2013; 50: 200-205.

[17] Srivastava S. P16INK4A and MIB-1: an immunohistochemical expression in preneoplasia and neoplasia of the cervix. Indian J Pathol Microbiol 2010; 53: 518-524.

[18] Alos L, Hakim S, Larque AB, de la Oliva J, Rodriguez-Carunchio L, Caballero M, Nadal A, Marti C, Guimera N, Fernandez-Figueras MT, Quint W and Ordi J. p16 overexpression in high-grade neuroendocrine carcinomas of the head and neck: potential diagnostic pitfall with HPV-related carcinomas. Virchows Arch 2016; 469: 277-284.

[19] Han CP, Kok LF, Wang PH, Wu TS, Tyan YS, Cheng YW, Lee MY and Yang SF. Scoring of p16(INK4a) immunohistochemistry based on independent nuclear staining alone can sufficiently distinguish between endocervical and endometrial adenocarcinomas in a tissue microarray study. Mod Pathol 2009; 22: 797-806.

[20] Pandey M, Bhosale PG and Mahimkar MB. Detection of HPV E6/E7 mRNA in clinical samples using rna in situ hybridization. Methods Mol Biol 2018; 1726: 167-175.

[21] von Knebel Doeberitz M, Rittmuller C, Aengeneyndt F, Jansen-Durr P and Spitkovsky D. Reversible repression of papillomavirus oncogene expression in cervical carcinoma cells: consequences for the phenotype and E6-p53 and E7-pRB interactions. J Virol 1994; 68: 2811-2821.

[22] Yoshimatsu Y, Nakahara T, Tanaka K, Inagawa Y, Narisawa-Saito M, Yugawa T, Ohno SI, Fujita M, Nakagama H and Kiyono T. Roles of the PDZ-binding motif of HPV 16 E6 protein in oncogenic transformation of human cervical keratinocytes. Cancer Sci 2017; 108: 1303-1309.

[23] Yemelyanova A, Ji H, Shih IeM, Wang TL, Wu LS and Ronnett BM. Utility of p16 expression for distinction of uterine serous carcinomas from endometrial endometrioid and endocervical adenocarcinomas: immunohistochemical analysis of 201 cases. Am J Surg Pathol 2009; 33: 1504-1514.

Table S1. The antibodies used in this study

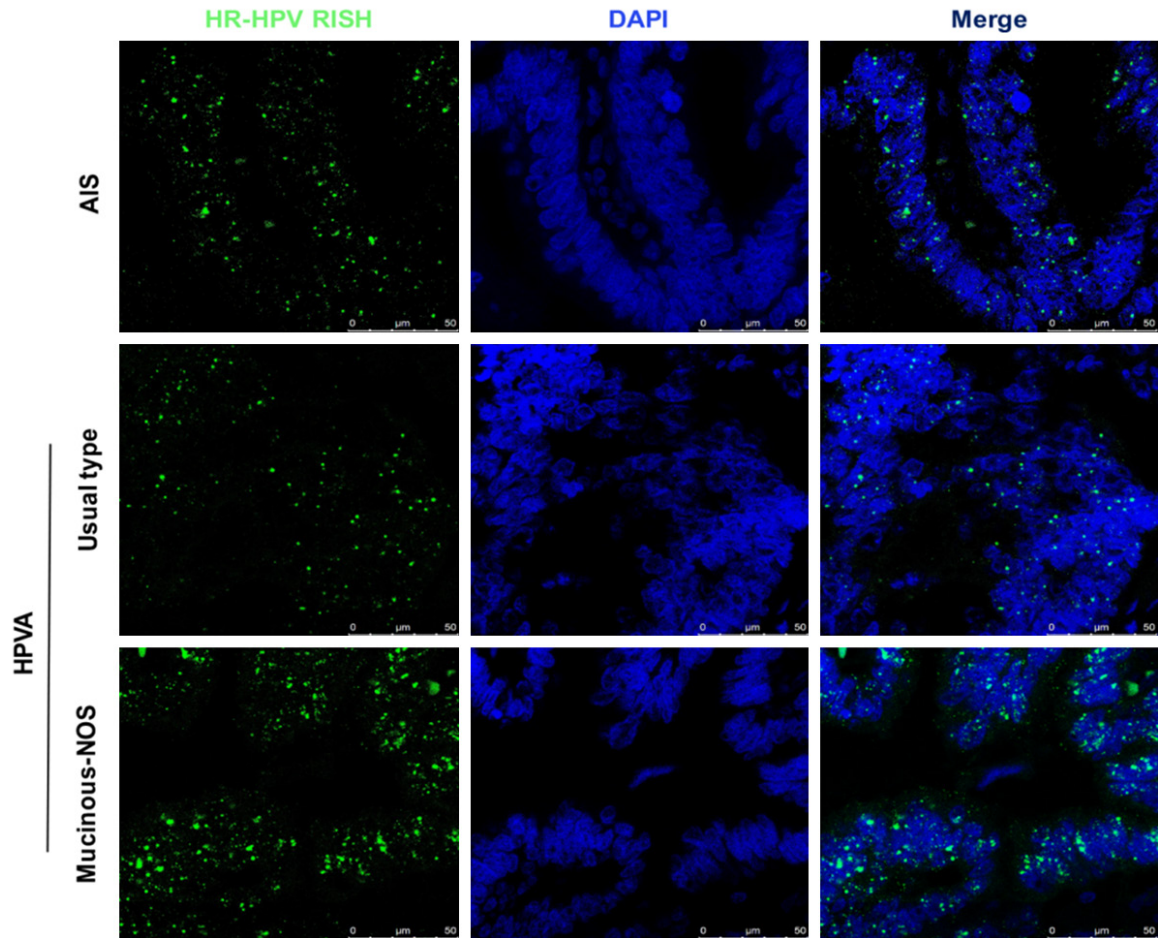| Antibodies	Dilution	CLONE	Manufacturers
p16^{INK4a}	1:200	E6H4	Roche
Ki67	1:100	MIB-1	Dako
p53	1:1000	FL-393	Santa Cruz
Napsin-A	1:200	IP64	Novocastra
HNF-1β	1:2000	EPR18644-13	Abcam

Figure S1. HR-HPV RISH performances in the HPVAs by fluorescence. The fluorescence representative images of HR-HPV RISH expressions in the AIS, adenocarcinoma of usual type and adenocarcinoma of mucinous-NOS type. Scale bars = 50 μm. The fluorescent signals of HR-HPV were stained by green (Fluor 488). DAPI was used to staining for the nucleus. AIS: adenocarcinoma in situ; NOS: not otherwise specified.
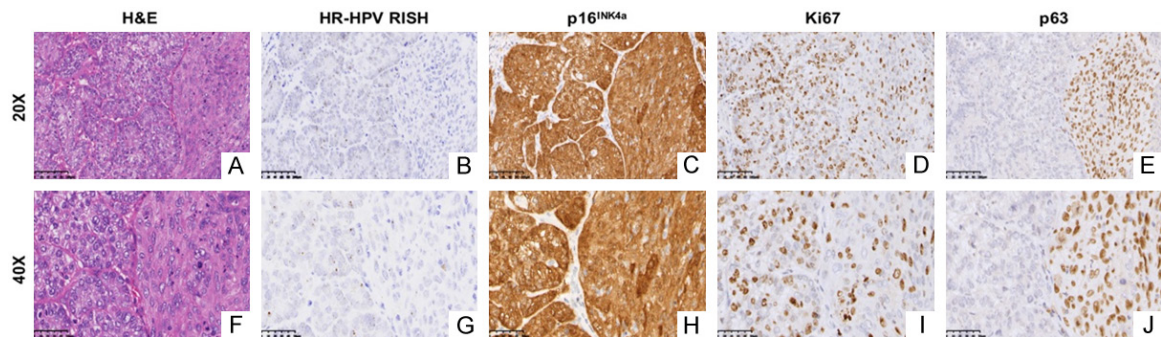

Figure S2. HR-HPV RISH, p16^{INK4a}, Ki67 and p63 performances in 21 cases of endocervical adenosquamous carcinoma. The representative images of H&E, HR-HPV RISH, p16INK4a, Ki67 and p63 expressions in the endocervical adenosquamous carcinoma. A-E: Scale bars = 100 μm. F-J: Scale bars = 50 μm.
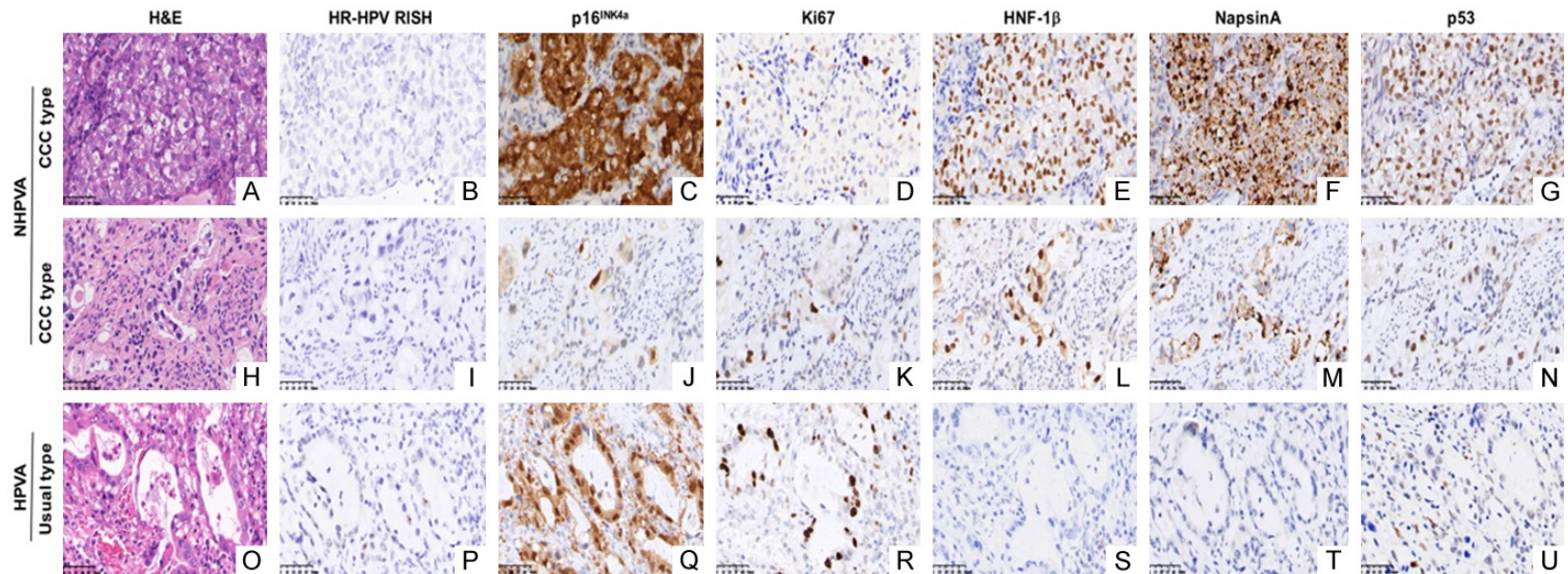
Figure S3. The HNF-1β and Napsin-A performances in the NHPVA of clear cell type and HPVA with similar morphology. The representative images of H&E, HR-HPV RISH, p16INK4a and Ki67 expressions in the NHPVA of clear cell type (A-N) and the HPVA with similar morphology (O-U). p53 (G, N and U), HNF-1β (E, L and S) and Napsin-A (F, M and T) were used to confirm the CCC type. The expressions of p16INK4a (C and J) were various in the NHPVA of clear cell type. Scale bars = 50 μm. NHPVA: non HPV-associated adenocarcinoma. HPVA: HPV-associated adenocarcinoma.